Effects by Different Microstructure and Texture of Hot Band on the Evolution of Microstructure and Texture after Cold Rolling and Final Annealing of Ferritic FeSi Steels

A. Franke[1], J. Schneider[2], B. Bacroix[3] and R. Kawalla[2]

[1]*Stahlzentrum Freiberg e.V., Leipziger Straße 34, 09599 Freiberg, Germany*

[2]*Institute of Metal Forming, Technische Universität Bergakademie Freiberg, Bernhard-von Cotta-Str.4, 09596 Freiberg, Germany*

[3]*LSPM – CNRS, UPR3407, Université Paris 13, 99, Av. J.B. Clément, 93430 Villetaneuse, France*

Abstract: It is well established that there is an interplay and interaction between the processing steps at fabrication of non-oriented electrical steels: hot rolling, cold rolling and annealing with respect to the evolution of the microstructure and texture. In this paper we will analyse in detail by optical microscopy and EBSD-measurements the influence of the microstructure of hot band prepared in different ways on the deformation structure after cold rolling and finally the evolution of microstructure as well as texture at final annealing due to recrystallization followed by grain growth. It will be demonstrated that the microstructure of the hot band effects the start of the recrystallization and finally the start of the grain growth at final annealing. The evolution of the microstructure at the stage of recrystallization is rather inhomogeneous across the thickness. This results from the complex deformation substructures after cold rolling. It will be pointed out that an explanation of the texture evolution at recrystallization only by in-plane compression stress fails. The inclusion of shear stress may explain the observed figure for the texture. The grain growth, which is necessary for the non-oriented electrical steels to reach the desired low values of specific magnetic losses, is finally the dominant process at the relevant higher annealing temperatures. The evolution of texture at recrystallization is different from those at grain growth.

Keywords: Ferritic FeSi, Hot Rolling, Cold Rolling, Annealing, Deformation Structure, Microstructure, Texture.

1. INTRODUCTION

It is well established that there is an interplay and interaction between the processing steps at fabrication of non-oriented electrical steels: hot rolling, cold rolling and annealing with respect to the evolution of the microstructure and texture [1-3]. Depending on the microstructure of the hot band a rather complex deformation structure appears for ferritic FeSi steels after the heavy cold rolling to reach the desired final thickness [4, 5]. This complex microstructure affects the ongoing recrystallization and evolution of microstructure and texture at final annealing [6-8].

In this paper we will analyse in detail by optical microscopy and EBSD-measurements the influence of the microstructure of hot band prepared in different ways on the deformation structure after cold rolling and the evolution of microstructure as well as texture at final annealing due to recrystallization followed by grain growth. We will regard mainly only ferritic FeSi steel with 2.4 wt. of Si. First, we will summarize the obtained different image for the microstructure of the hot strip before cold rolling and the resulting microstructure after

cold rolling. The hot band of ferritic FeSi2.4 with a thickness of 2 mm were prepared by variation of the conditions at hot rolling and at cooling after finishing the hot rolling. Hot band with an additional hot band annealing before cold rolling were also regarded. We will analyse the resulting microstructure and texture at final annealing of these cold rolled material with different deformation structure. Thereby we will focus on the effect of annealing temperature, respectively annealing time on the evolution of microstructure and texture. The ongoing processes: recrystallization followed by grain growth will be differentiated. The mechanism for the texture evolution at recrystallization will be discussed. The texture evolution during grain growth, which follows the recrystallization will be also regarded.

It will be demonstrated that the microstructure of the hot band effects the start of the recrystallization and finally the start of the grain growth at final annealing. The evolution of the microstructure at the stage of recrystallization is rather inhomogeneous across the thickness. This is caused by the complex deformation structure after cold rolling. It will be pointed out that an explanation of the texture evolution at recrystallization only by in-plane compression stress fails. The grain growth, which is necessary for the non-oriented electrical steels to reach the desired low values of

specific magnetic losses, is finally the dominant process at the relevant higher annealing temperatures. The evolution of texture at recrystallization is different from those at grain growth.

2. EXPERIMENTAL

The different hot rolled materials were prepared using the four stand pilot line for hot rolling at the Institute of Metal Forming, TU Bergakademie Freiberg (IMF). Thereby the hot rolling finishing temperature as well as the conditions of coiling after finishing the hot rolling are varied. In addition, some samples were annealed (hot strip annealing) before cold rolling in a separate processing step.

Table **1** gives an overview of the samples, which were regarded in this paper. Cold rolling (CR) of the hot rolled strip with a thickness of 2 mm to a thickness of 0.5 mm was realized on a two-high stand at the IMF with four passes. Final annealing was carried out in an annealing furnace by which it is possible to simulate the mostly used commercial continuously annealing process at temperatures up to 1050 °C for 20 s. The heating rate was about 30 °C/s and the cooling rate was about 15 °C/s. In addition, box annealing (lower temperatures and longer annealing time) was done. The microstructure and texture before and after cold rolling was observed by optical microscopy and EBSD. The ongoing changes of the microstructure and texture at final annealing were analyzed by the orientation imaging microscopy (OIM), the image quality as well as image quality plus rotation angle map (IQ plus misorientation), and the distribution function of the misorientation vs. angle obtained from EBSD measurements. General features of the microstructure of hot strips can be classified in three

types: equiaxed grains with different sizes, pancake grains and bands, see [9]. The resulting deformation substructures after cold rolling were classified following the classification in [10]. One may distinguish deformation bands, shear bands, transition bands.

The ongoing structural processes at final annealing were described following the definition of recovery and recrystallization given in [11, 12]. Straight recovery is characterized by the formation of subgrain structures with low angle grain boundaries, which leads to no change of the texture. Recrystallization comprises the appearance of nucleus and the formation of small grains. The appearance of large angle grain boundaries is taken as indicator for recrystallization. Grain growth, which occur at higher annealing temperatures, respectively longer annealing time, is defined as grain coarsening after completed recrystallization (stress less polycrystalline microstructure).

Texture is studied in detail by the $\varphi_2=45°$ section of the orientation distribution functions (ODFs). Figure **1** shows the main fibers and components in the $\varphi_2=45°$ section of the orientation distribution functions (ODFs), which we will particular view. To study the inhomogeneous nature of microstructure and texture across the thickness we will analyze also certain areas within the samples.

3. RESULTS

3.1. Microstructure and Texture of the Hot Rolled and Cold Rolled Material

3.1.1. Hot rolled Material

Due to the variation of the parameters at final hot rolling: starting temperature and finishing temperature

Table 1:   Hot Rolled Samples Prepared at IMF of Ferritic FeSi Steels

Sample	Thickness	HR: Starting Temperature	HR: Finishing Temperature	Annealing Temperature and Time at Cooling
1	2mm	960°C	820°C	Quenching to 400°C
2	2mm	1090°C	860°C	750°C/20min
3	2mm	1150°C	770°C	Air Cooling to RT
4	2mm	1010°C	930°C	750°C/75min
5	2mm	1250°C	1000°C	750°C/270min
6	2mm	1010°C	960°C	750°C/240min
7[**]	2mm	1150°C	770°C	Air Cooling to RT
8[**]	2mm	960°C	820°C	Quenching to 400°C
9[**]	2mm	1250°C	1000°C	750°C/270min

[**]Additional hot band annealing in a separate processing step before cold rolling:
Sample 7 –Sample 3 annealed at 850°C/20min; Sample 8 – Sample 1 annealed at 900°C/2min; Sample 9 – Sample 5 annealed at 900°C/2min.

and the type of cooling after the last pass at hot rolling, respectively the thermal treatment immediately after the last pass, one gets a variety of images for the microstructure after hot rolling. In addition the number of passes and deformation per pass effects the resulting microstructure and texture.
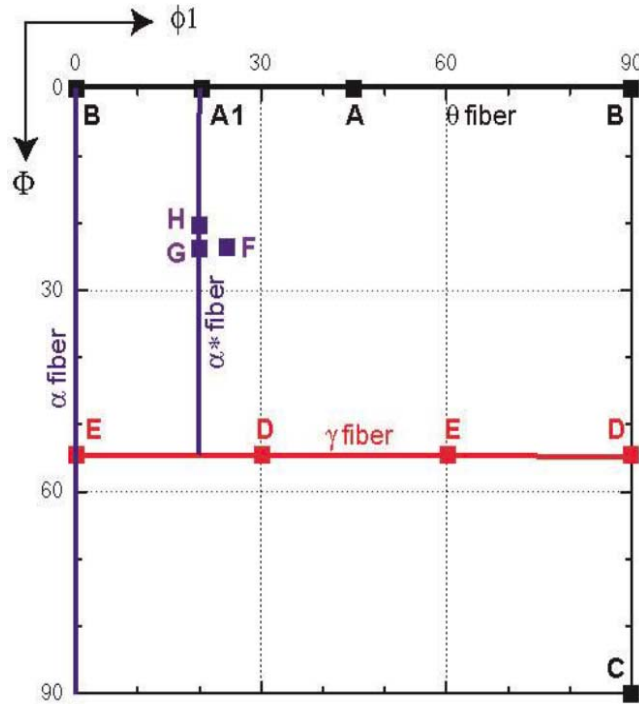
Figure 1: φ_2 = 45°section of ODF.

Cube fibre (θ- fibre) - <001>parallel ND; α- fiber <110> parallel RD; γ - fibre <111> parallel ND, α* - fibre {h,1,1}<1/h,1,2>, A – {100}<001> cube texture, A$_1$ = {100}<012>, B –100}<110> rotated cube texture, C – {110}<001> Goss texture; D - component {111}<112> of the γ – fibre; E – component {111}<121>, F – {113}<251>; G - component {113}<136> of the α* - fibre ; H – component {411}<148> of the α* - fibre, F = {113}<251>, G = {113}<136>, H = {411}<148>.

Figure **1** presents the optical micrograph for the total cross section of some of the samples on the Table **1** before cold rolling, which were fabricated at different hot rolling conditions. Figure **2** shows the optical micrograph for sample 7 and 8, which were in addition annealed before cold rolling (hot strip annealing).

The OIM (Orientation Image Map) obtained from EBSD measurements illustrated in addition the microstructure (grain structure) and the present texture components across the thickness. Figures **3** and **4** presents the OIM of samples 1, 2 and 5 as well as of samples 7, 8 and 9, which were annealed in an additional processing step (hot strip annealing). The texture components, which are indicated by OIM are

more explained in Figure **6**. In the OIM the notation 111, 001, 101 are connected with the crystal reference system. Thereby we have blue -111 parallel ND (gamma fibre) and red – 100 parallel ND (cube fibre). ND gives the normal direction of the sample.

A more detailed insight in the figure for the texture in the hot strips before cold rolling is given in Figure **7**, which presents the ODFs.

Summering the obtained results, presented in Figures **2** to **7**, a rather complex and inhomogeneous figure for the microstructure and texture across the thickness is found. The obtained figure depends very sensitive on the parameters at fabrication of the hot strip.

It should be remarked, that the obtained features for the hot strip samples, which were prepared using the four stand pilot line for hot rolling at the Institute of Metal Forming TU Bergakademie Freiberg (IMF), are similar and representative for the resulting microstructure using a commercial hot rolling line, see Figure **8**.

Nowadays, an additional hot band annealing before cold rolling is widely used to produce higher permeability grades commercially. An additional hot band annealing in a separate processing step before cold rolling leads to a decrease of the magnetically disadvantageous Gamma fibre and of the α – fibre as well as an increase of the magnetically preferable cube fibre texture and α*-fibre in the finally annealed non-oriented electrical steels, see also [13, 14]. An analysis of the preferable magnetic textures of non-oriented electrical steels is given in [15].

For these reasons, it is interesting to have a look on the effect of different fabrication routes of the hot strip on the resulting texture in the hot strip. From Figure **7** it can be seen that at rapid quenching after the last pass of hot rolling (sample 1) the intensity of the α – fibre is large. Even the intensity of the Gamma fibre is relatively large. A similar figure is obtained for sample 3. A thermal treatment immediately after the last pass at hot rolling, see sample 2 in Figure **7**, results in an remarkable decrease of the Gamma fibre. A high intensity of the preferable magnetic texture components, high intensity of cube fibre and α*-fibre, is reached for sample 2. A similar figure like for sample 2 is observed for sample 7, which were annealed in a separate processing step (hot band annealing). The obtained figure of the ODF for sample 8 and 9, which
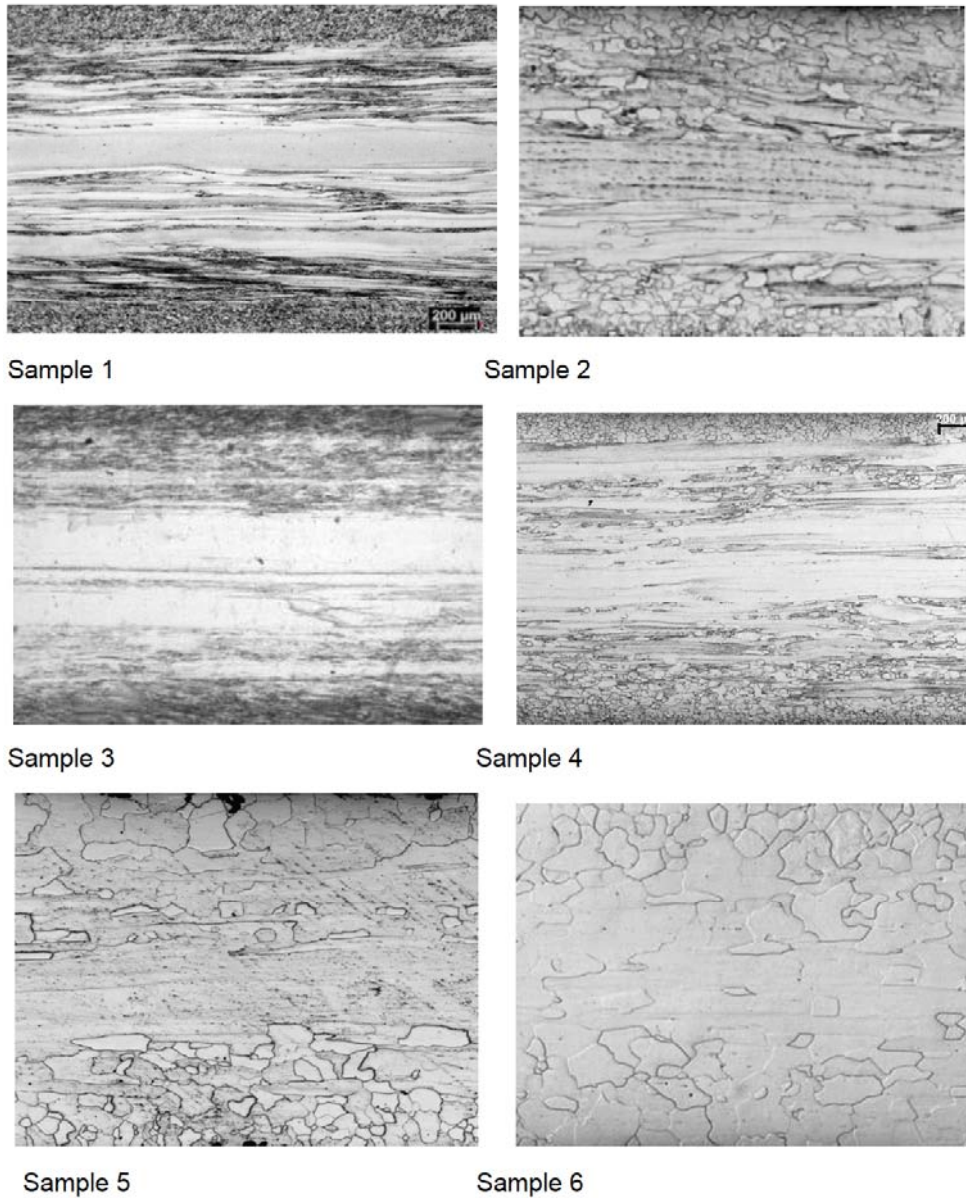
Figure 2: Optical micrograph for the total cross section of samples 1 to 6 before cold rolling; thickness before CR 2.00 mm; size scale is for all samples the same.
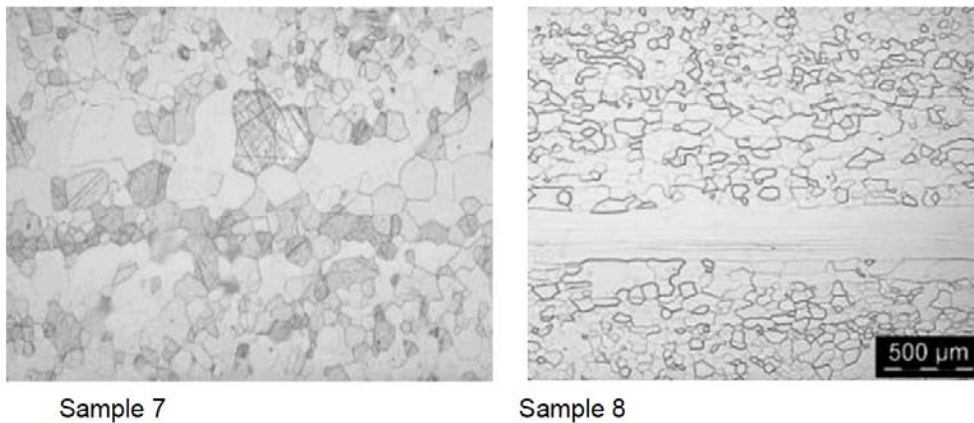
Figure 3: Optical micrograph for the total cross section of samples 3 and 1, which appeared a hot strip annealing in a separate processing step before cold rolling; size scale is the same (Sample 7 – sample 3 annealed 850°C/20min ; Sample 8 – sample 1 annealed 900°C/2min).
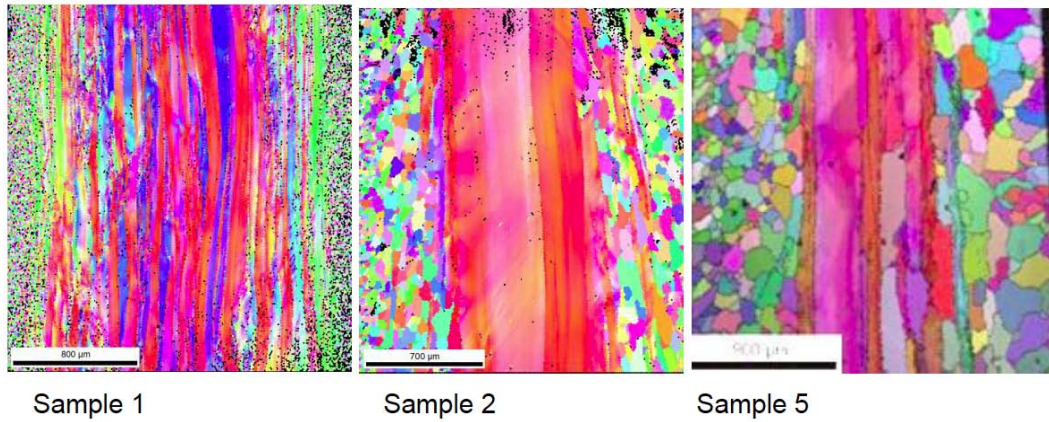
Figure 4: Orientation Image Map (OIM) of sample 1, 2 and 5 after HR.
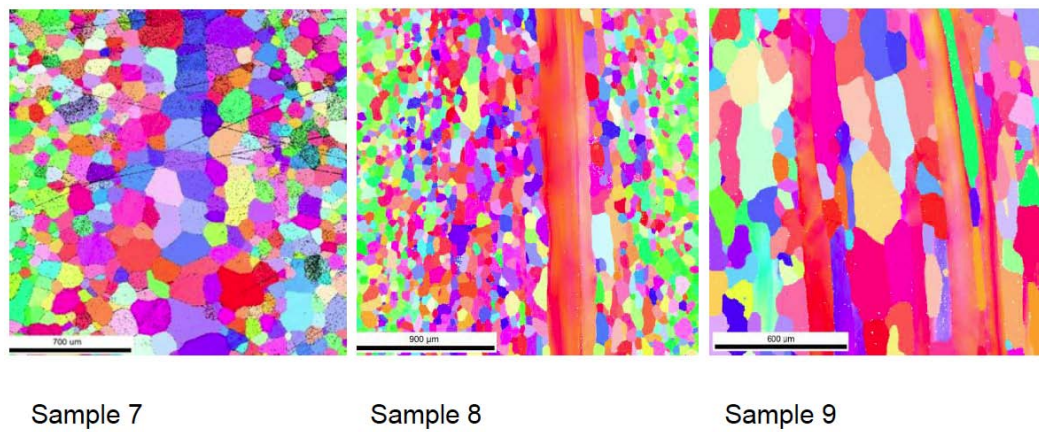
Figure 5: Orientation Image Map (OIM) of sample 7, 8 and 9 after Hot Rolling (all samples were annealed in a separate step before cold rolling).
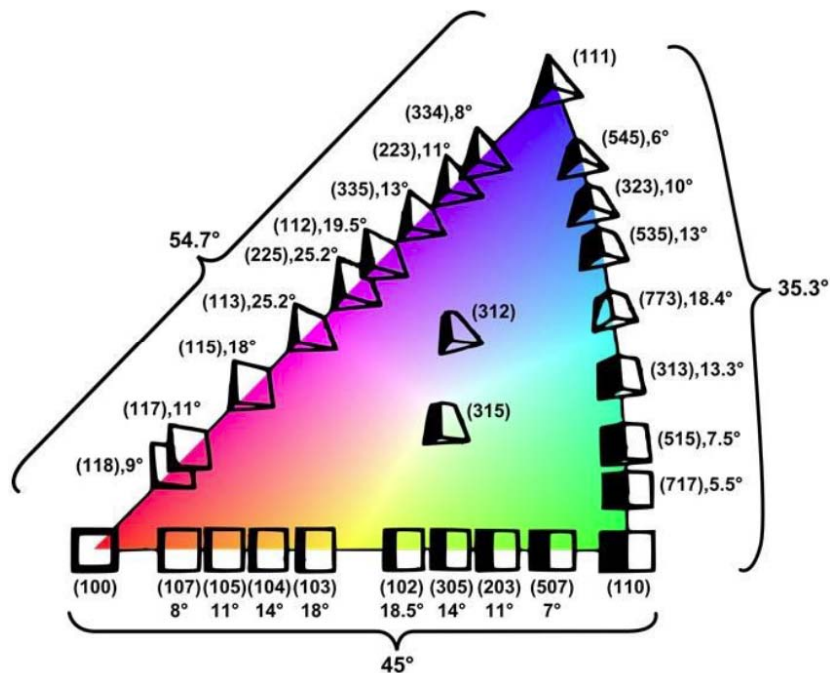
Figure 6: Texture components descried by OIM (from literature), see also: Journal of Material Science and Technology Research, 2018, 5, 28-38.
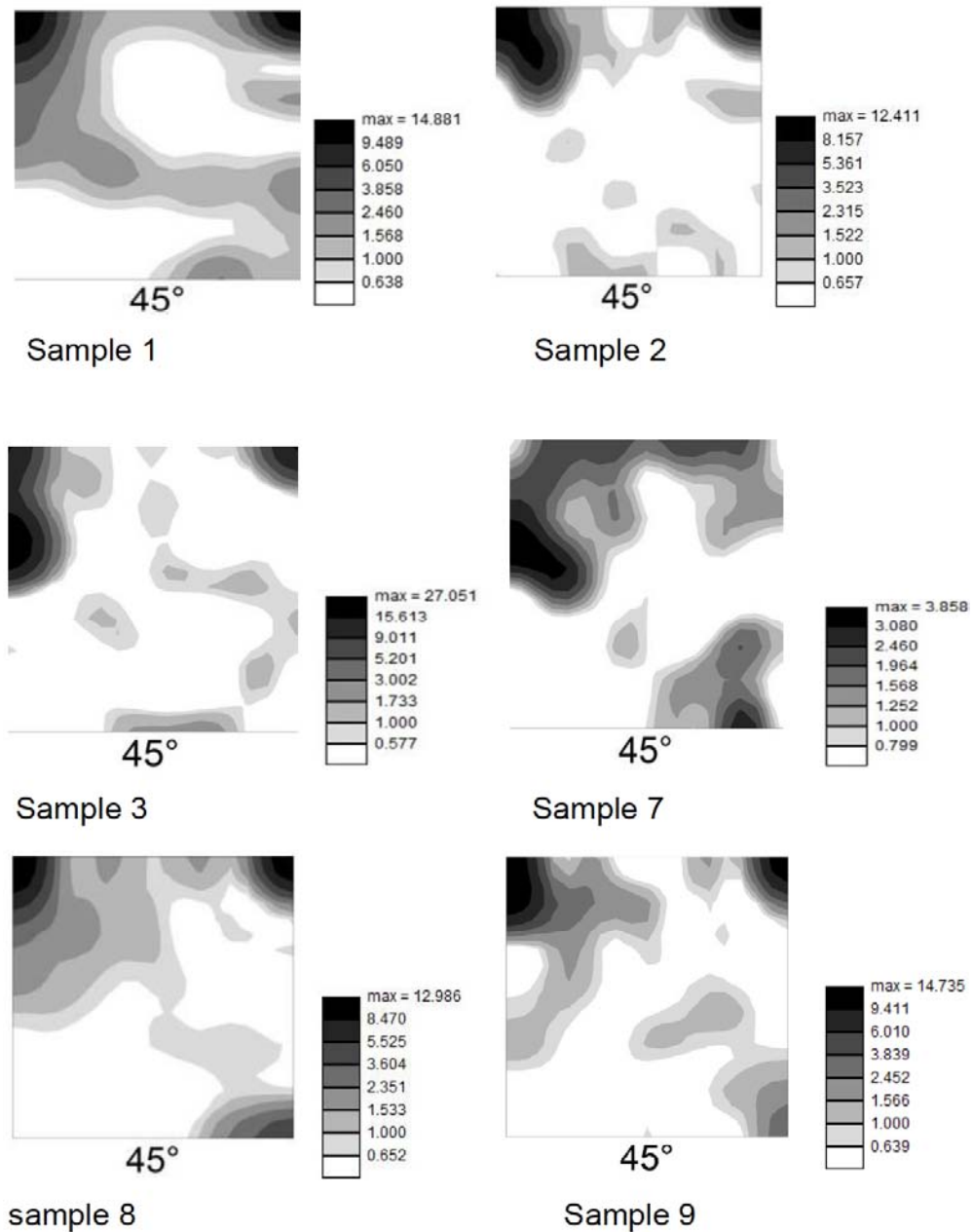
Figure 7: $\varphi_2=45°$ section of ODF for the whole cross section for the samples 1, 2, 3 and 7, 8, 9 before cold rolling.

were also annealed in a separate processing step (hot band annealing) exhibits a much less preferable magnetic texture intensity compared to sample 7. It reflects the fact that the result of an additional hot band annealing depends also remarkable on the microstructure of the hot strip after hot rolling and the annealing conditions at the process of hot band annealing in a separate processing step.

In summary, it appears that a high intensity of the preferable magnetic texture components may be reached in two ways. First by an additional hot band annealing in a separate processing step. Second by an optimum annealing (appropriate finishing temperature at hot rolling and cooling after the last pass) integrated in the process of the hot strip fabrication. Such an optimal annealing integrated into the process of the hot strip fabrication results in a specific microstructure, characterized by pancake grains, rather elongated grains and partly recrystallized regions.

3.1.2. Cold Rolled Material

Starting from the most common thickness of 1.8 mm to 2.5 mm of the used hot strip for non-oriented electrical steels a cold rolling with a high deformation is necessary to get the desired thickness of 0.35 to 0.65 mm.
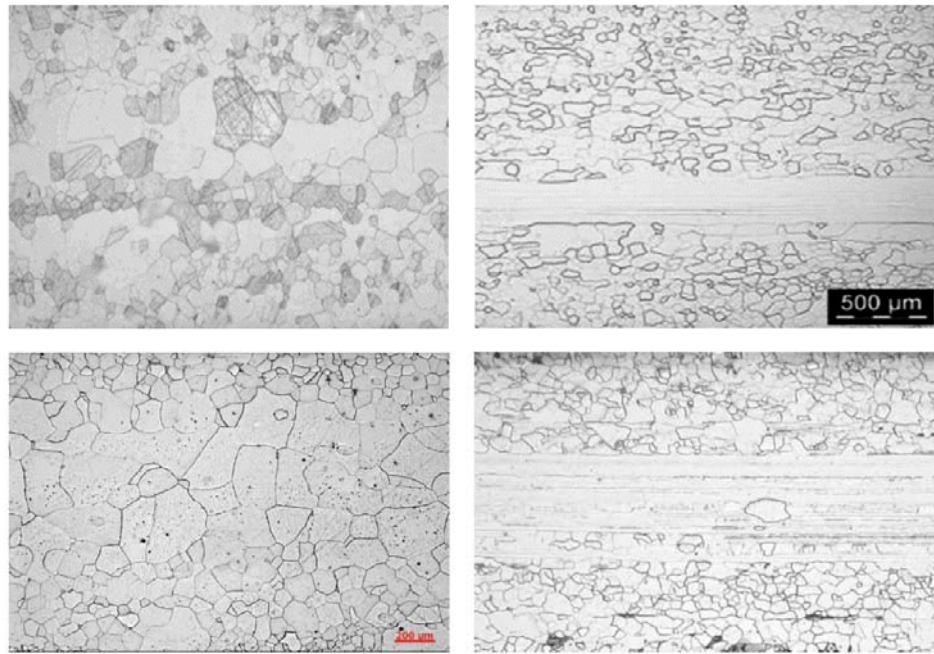
Figure 8: Optical micrographs for the total cross section of hot strips fabricated at the pilot line (above) and using a commercial line (below).

Sample 1   Sample 2   Sample 7
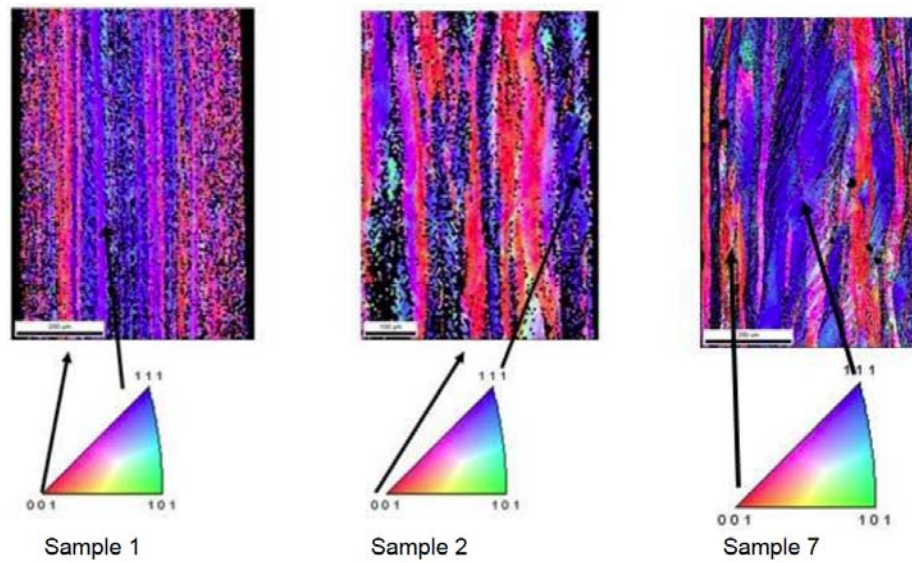
Figure 9: OIM of sample 1, 2 and 7 after cold rolling.

Figure 10: Optical micrographs after cold rolling; left: annealed immediately after the last pass at hot rolling; right – thermal annealing in a seperate processing step before cold rolling.
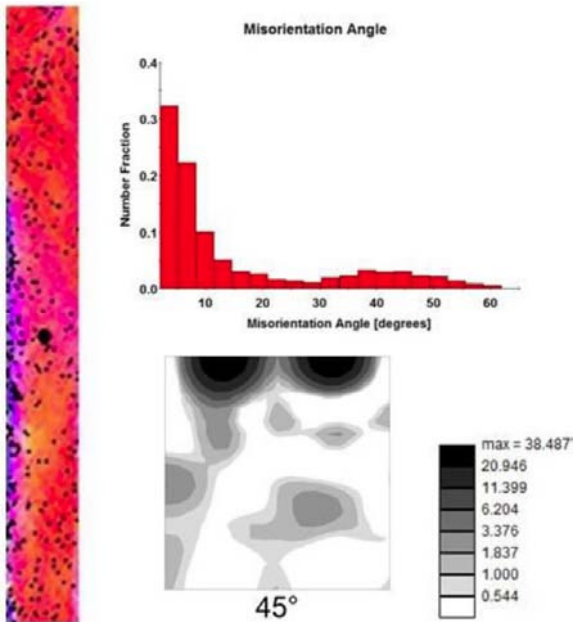
Figure 11: Sample 2 - band with cube fibre.
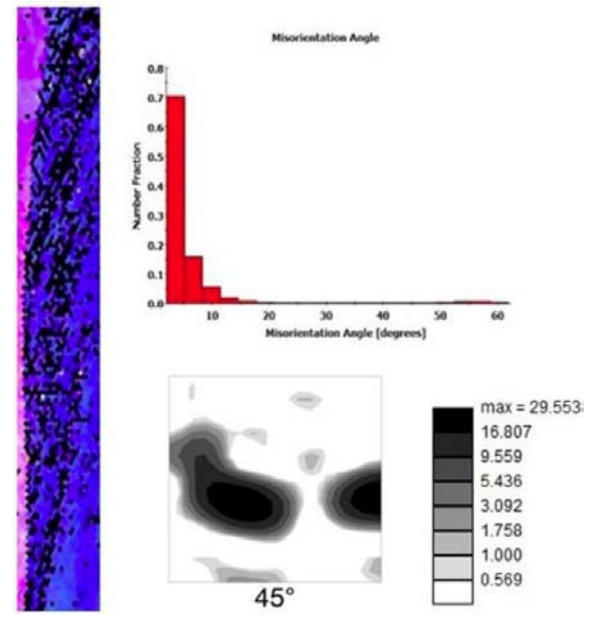
Figure 12: Sample 7 - band with with γ - fibre texture.

In our case we used hot strip of 2 mm and realized cold rolling to a thickness of 0.50 mm. Figure **9** presents the OIM for the samples 1, 2, and 7. One finds a rather complex deformation structure, which depends on the microstructure of the hot strip, see also [4, 5]. The OIM indicate the presence of bands oriented mainly in the rolling direction with γ- fiber texture (<111>parallel NR) as well as bands with cube fiber texture (<001>parallel ND), called deformation bands, distributed more or less over the thickness. Thereby the portion of the area with γ- fiber texture seems to be larger for the sample with an additional hot strip annealing before cold rolling (sample 7). A high intensity of shear bands is visible in the areas with γ - fiber texture (<111>parallel NR) for this sample.

Shear bands across the thickness are very clear visible in the optical micrographs for any samples, which suffered a thermal treatment immediately after the last pass after hot rolling or after a thermal treatment in a separate processing step before cold rolling (hot band annealing). Typical examples are given in Figure **10**. Shear bands are described as highly effective sites for nucleation at recrystallization [10]. Shear bands may be identified as linear lines with low IQ. EBSD pattern becomes worse in the case of crystal lattice distortion [16].

The rather inhomogeneous deformation structure and the quite different local microstructure and texture across the thickness, which were already described in [4], will affect the ongoing recrystallization process at

final annealing of the cold rolled material. The information on this may give some hints for the mechanism at recrystallization: appearance of nuclei and the formation of small grains.

For that reason, we will add in this paper even more details. Figures **11** to **15** demonstrate for the sample 2 and 7 the local different figures for the texture. The Figures present the OIM, the ODF, the distribution function of the misorentation and in some cases the IQ (image quality) in different areas of the samples.

For bands with cube fibre texture, see Figure **11**, the distribution function for the misorientation exhibit a remarkable quantity of large angle grain boundaries, which may indicate locally recrystallization. For bands with γ- texture, see Figure **12**, we observe mainly low angles. The transition bands between the bands with cube, respectively γ- texture, exhibit a mixture of areas with quit different character of the misorientation angle and texture, see Figure **13**. The areas with shear line, which show mainly only large angle grain boundaries, may exhibit quite different character with respect to the texture, see Figures **14** and **15**.

3.2. Microstructure and Texture at Final Annealing

3.2.1. Annealing at Low Temperatures

The ongoing processes at annealing of the cold rolled strips with large deformation comprises at first the recovery and recrystallization. Straight recovery is characterized by the formation of sub grain structures
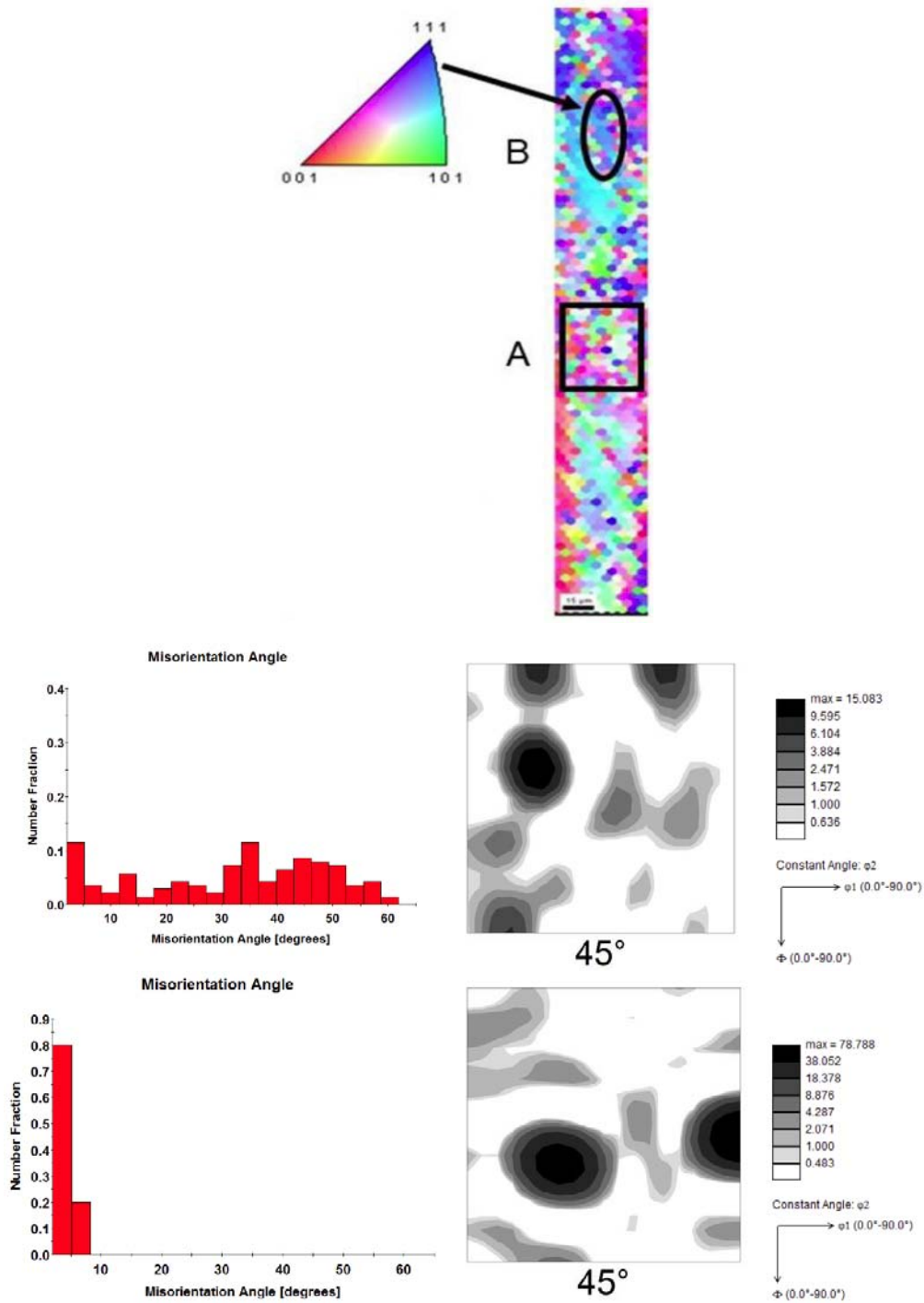
Figure 13: Sample 2 – transition bands: distribution function of misorientation vs. angle and the φ_2=45° section of the orientation distribution function for the areas A at the top and B at the bottom.

with low angle grain boundaries, which leads to no change of the texture. Recrystallization comprises the appearance of nucleus and the formation of small grains. Nucleation and movement of large angle grain boundaries characterize recrystallization. The appearance of large angle grain boundaries is taken as indicator for recrystallization. Figure **16** gives the image quality plus the rotation angle map (misorientation) of

sample 1 (left) and sample 2 (right) after annealing at 700 °C, 760 °C and 800 °C for 20 s. Figure **17** gives the misorientation distribution vs. angle of sample 1 and sample 2 after final annealing at 800 °C for 20s. Figure **18** presents the OIM for sample 1 and 2 after annealing at 700 °C, 760 °C and 800 °C for 20s.

The observed recrystallization process is rather inhomogeneous across the thickness and complex. As
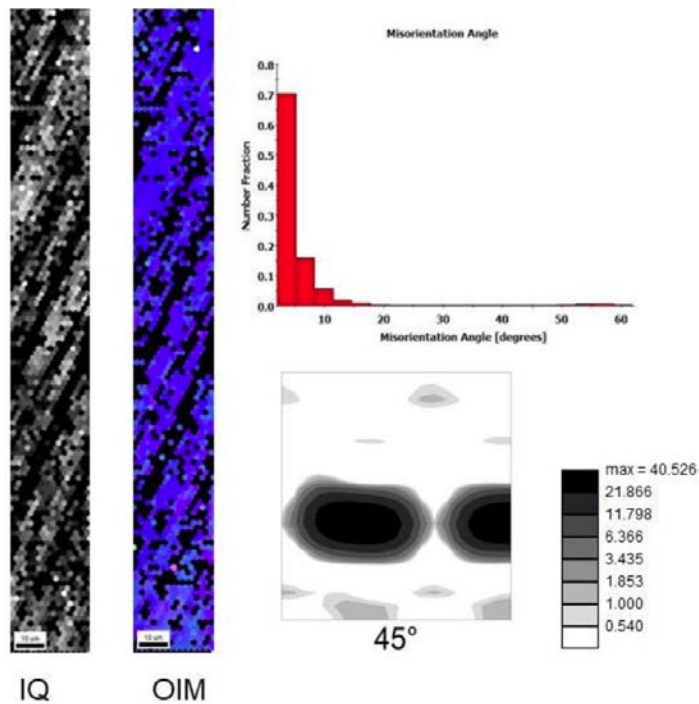
Figure 14: IQ, OIM, misorientation distribution function and the φ_2=45° section of the ODF for an area with γ- fiber texture of sample 7 after cold rolling, which contains shear bands.
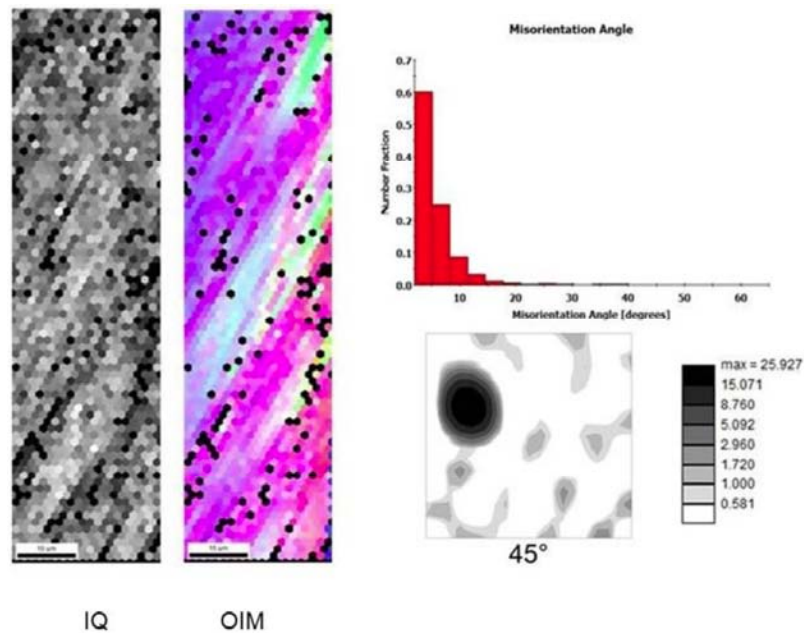
Figure 15: Sample 7- area with shear lines: IQ, OIM, distribution function of misorientation and the φ_2=45° section of the ODF.

can be seen from Figures **16** to **18** the microstructure of the hot strip determines the kinetic of the recovery and recrystallization at annealing after cold rolling.

Sample 1 was rapidly quenched after hot rolling, while sample 2 appeared a hot band annealed immediately after the last pass at hot rolling by variation of the cooling conditions. While for sample 2

the recrystallization is practically completed after annealing at 800 °C for 20s, one observes still a recovery for sample 1, characterized by an increase of the intensity of the misorientation at small angles. The different behavior may be correlated with the fact that sample 2 suffers an annealing immediately after the last pass at hot rolling, while sample 1 was rapidly quenched after the last pass. Similar tendency can be
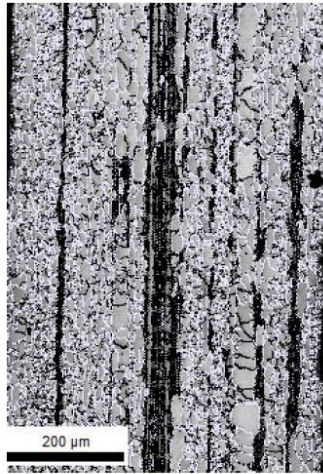
Sample 1; 700°C/ 20s

Sample 2; 700°C/20s
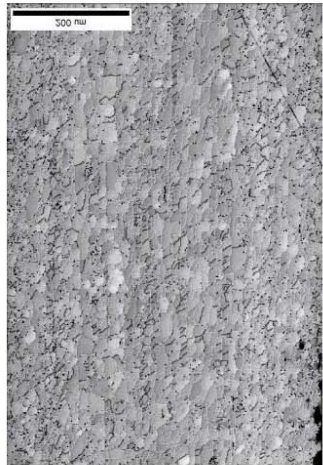
Sample 1 ; 760°C/20s
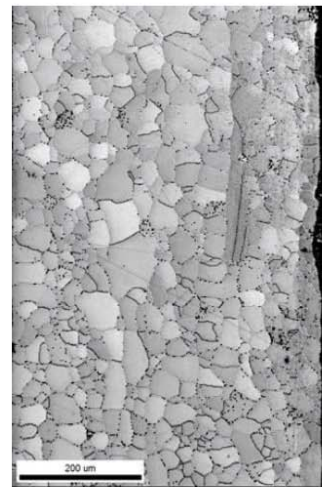
Sample 2 ; 760°C/20s

Sample 1; 800°C/ 20s
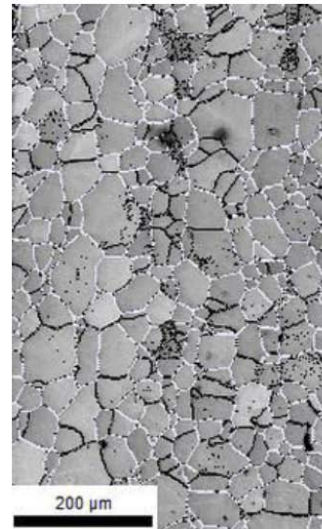
Sample 2; 800°C/20s

Figure 16: Image quality plus the rotation angle map (misorientation) of sample 1 (left) and sample 2 (right) after annealing at 700°C, 760°C and 800°C for 20 s; boundary rotation angle: black – 2° to 16°; white – 16° to 180°.
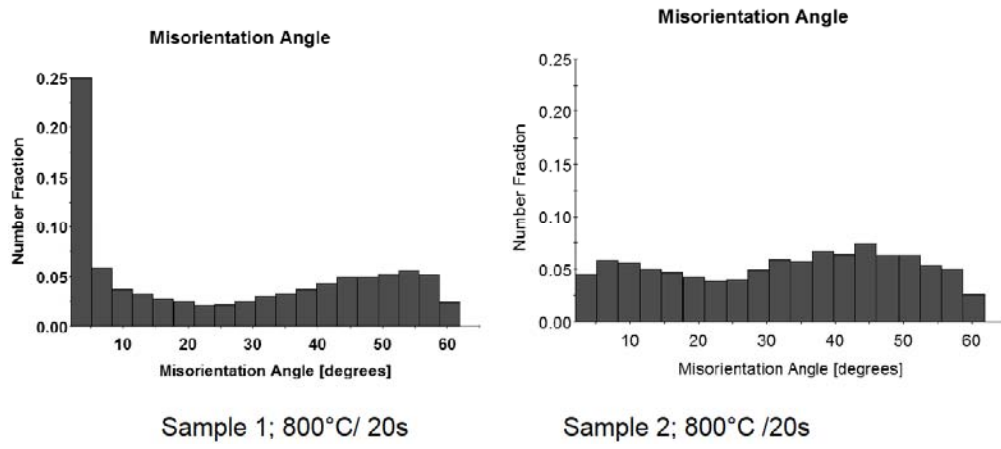
Figure 17: Misorientation distribution vs. angle of sample 1 and sample 2 after final annealing at 800°C for 20 s.
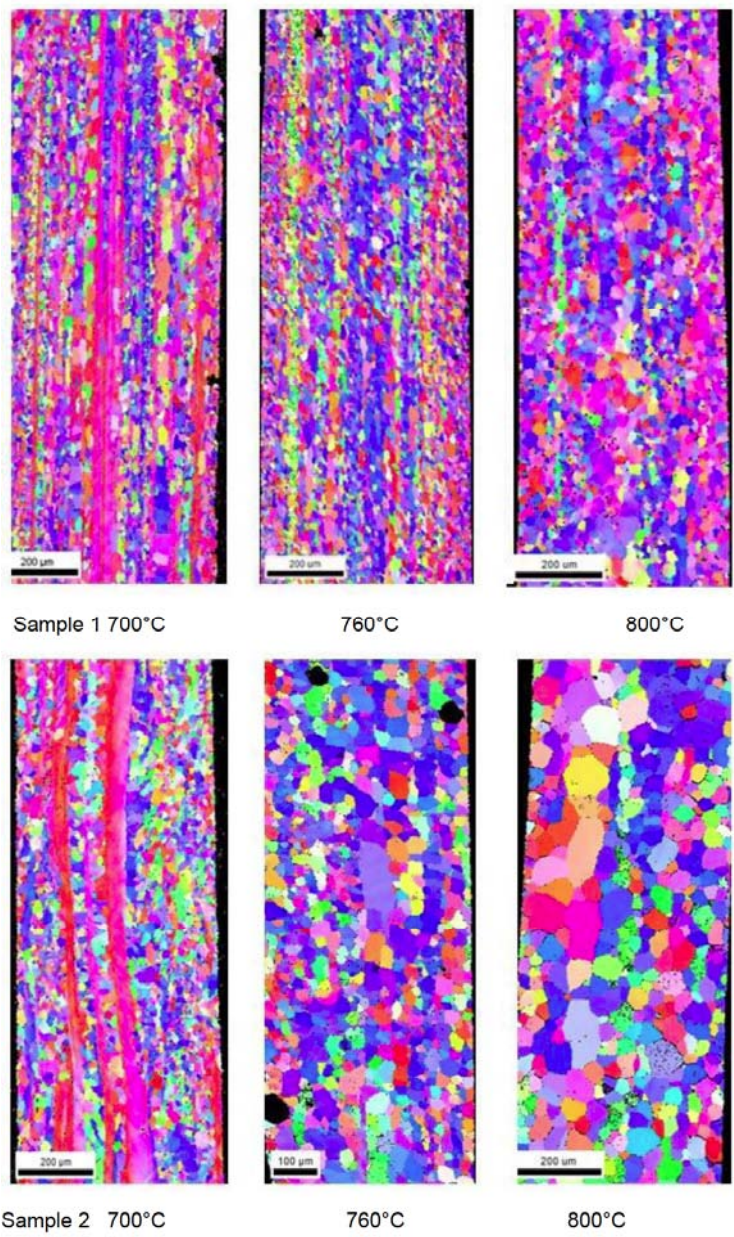
Figure 18: OIM of samples 1 and 2 after annealing at 700°C, 760°C and 800°C for 20s.
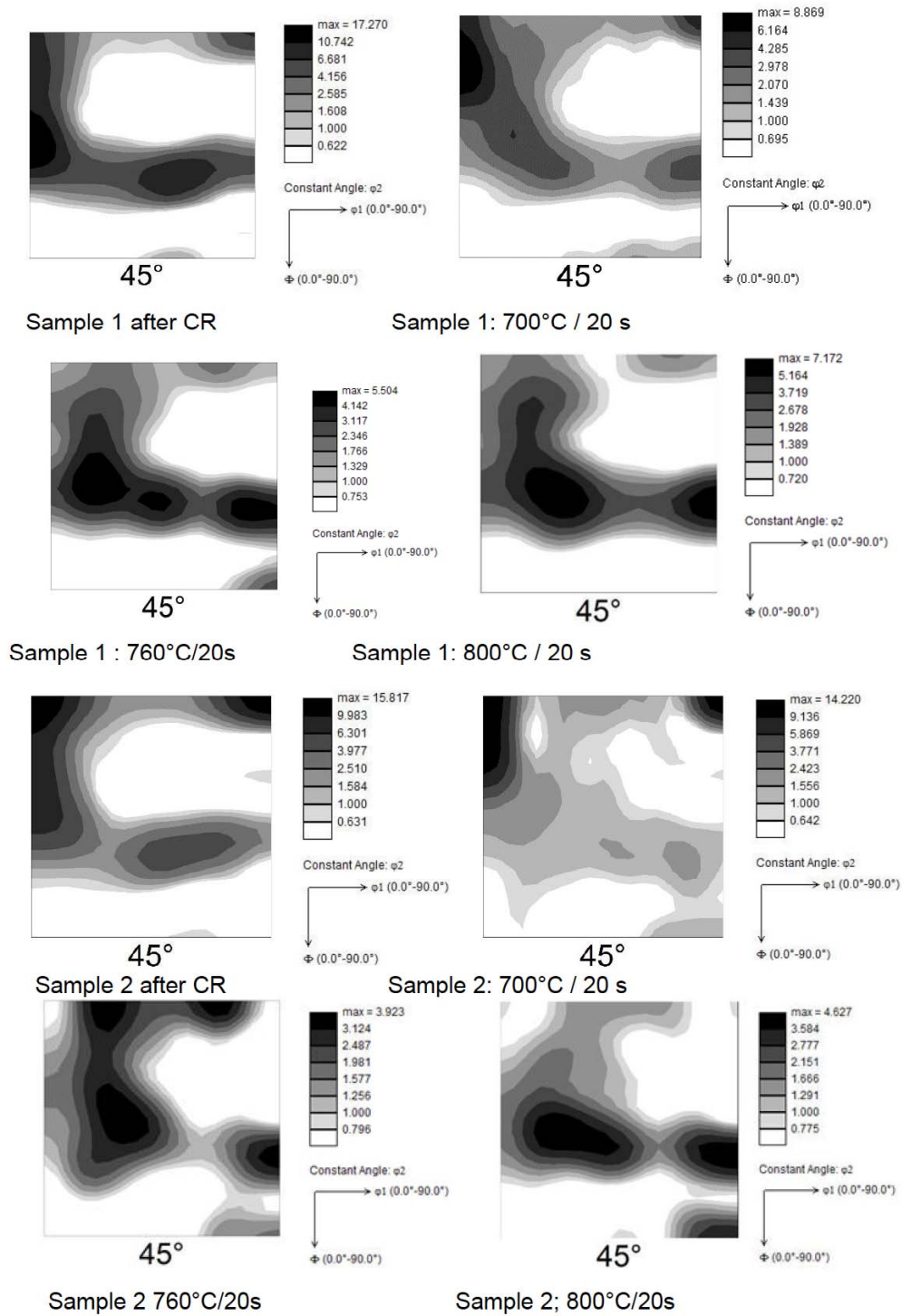
Figure 19: φ_2=45° section of the orientation distribution function for sample 1 and 2 after cold rolling and after annealing at different temperatures.

also seen for sample 3 (relative fast cooling after the last pass at hot rolling) and sample 7 (additional hot band annealing in a separate processing step before cod rolling). In all cases, the resulting microstructure is rather inhomogeneous across the thickness due to the fact that the ongoing processes are different across the thickness.

The changes in the intensities of the texture at annealing with temperatures, where recovery and recrystallization occurs, can be seen from the ODFs in Figures **19** and **20** for the samples 1 and 2, respectively for sample 3 and 7. To identify the texture components the angles are also given in Figure **19**. The alteration in the texture concerns not only a
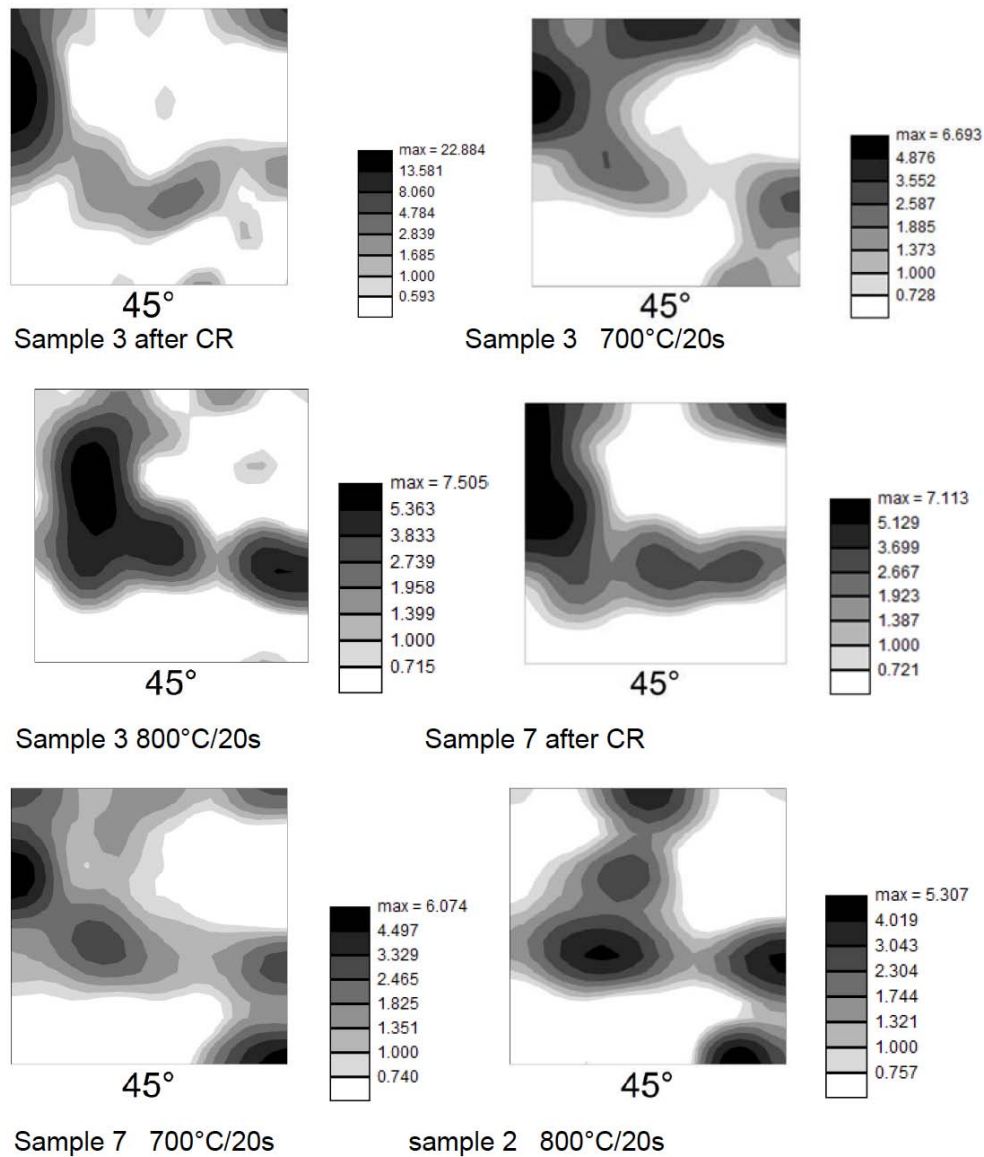
Figure 20: φ_2=45° section of the orientation distribution function for sample 3 and 7 at different temperatures.

decrease of the α – fibre texture and an increase of the Gamma – fibre texture, but also an increase of the cube fibre texture as well as the α* - fibre texture. Again, the evolution of the texture is different like the evolution of the microstructure for different hot strips. As described in [17], the large intensity of the α* - fibre texture in nonoriented electrical steels appear, if a very strong α - fibre and/or strong maximum on the rotated cube component is present in the cold rolled state.

The recrystallization texture may be explained based on the orientation dependence of the stored energy at cold rolling. The stored energy represents the driving force at annealing. It is generally assumed that cold rolling can be approximated by plane strain compression. The Taylor factor M, calculated within the Taylor theory of plastic deformation, my be taken as a

measure of the stored deformation energy [18]. For plain strain compression one finds for the orientation dependence of the stored energy [19] that a component of the α – fibre (110)<110> and the Gamma fibre have the largest values. The Goss component and the rotated cube component have the lowest values.

Following the concept of "high stored deformation energy" for the evolution of the recrystallization texture (Taylor factor M - measure of the stored deformation energy) the assumption of an in-plane strain compression gives a decrease of α - fibre and an increase of γ - fibre texture at annealing. It comes out that the really observed features for the recrystallization texture for the regarded ferritic FeSi cannot be explained assuming cold rolling can be approximated by plane strain compression as seen from the results
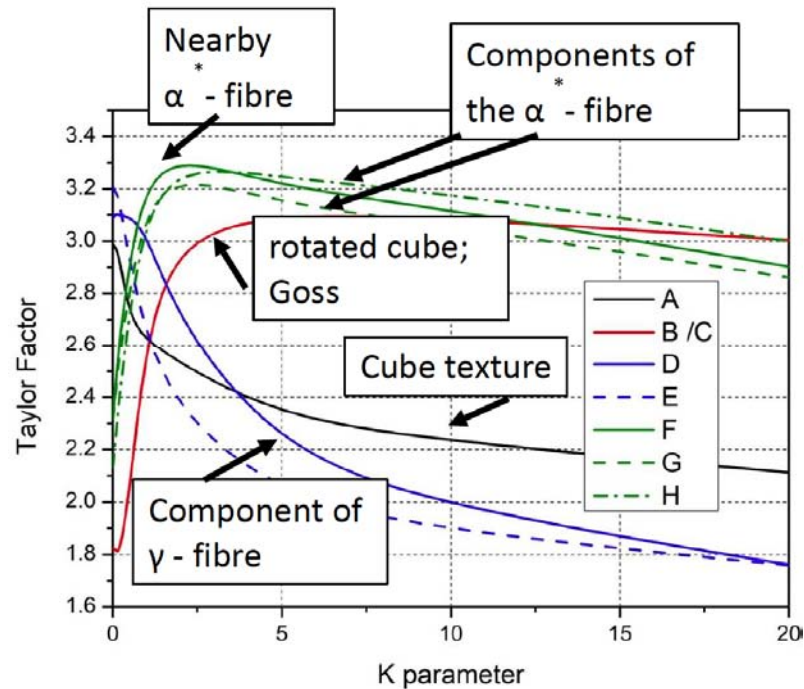
Figure 21: Taylor factor as function of the K (K characterize the shear stress).

for the microstructure and texture after cold rolling shear stress appears to a large extent.

The inclusion of shear stress in the concept of "High Stored Deformation Energy" will change the resulting "Taylor Factor Map" in the ODF $\varphi2$ –section, see Figure **21**. The parameter K – parameter characterize the shear stress (K = 0 only plane strain compression). We have an inversion of soft and hard components for K ≥1 (Hard components – large M factor; soft components – small M factor). When K ≥ 5, there is a complete inversion, since the rotated Cube (B) and Goss (C) orientations become the hardest, whereas the {110}<110> orientation and the γ fiber become the softest components.

Following the concept of "high stored deformation energy" as responsible mechanism for the texture evolution at recrystallization the presence of shear stress beside in-plane compression stress may induce nucleation of components of the cube fibre and α* fibre as well as Goss texture and rotated cube texture. This

is just what we observed in our case. It should be remarked that the recrystallization process comprise the appearance of nuclei on one hand and their growth to small grains on the other hand. Following the argument that high energy regions (high energy blocks) disappear first, the appearance of nuclei and their growth to small crystallites (subgrain growth) may be explained by the Taylor model (including shear stress). With respect to the formation of small grains by subgrain growth or grain coalescence (nucleation - high stored energy mechanism) we may have also strain induced boundary motion (SIBM - Bulging), growth of low-stored energy crystallites in high-stored energy crystallites [20]. Such SIBM (strain induced boundary motion) is described by Hutchinson [10] that in his way the new grain formed by heating must be thermodynamically stable locally and in this respect is a "low energy block". In summary, we may expect at recrystallization SIBM in soft components (low value of M) and nucleation in hard components (large values of M).

Table 2:   Mechanism of Recrystallization for Sample 1 and 2

Sample	1	2
Deformation bands (K = 0)	Rot. Cube (Low M_g) => SIBM Cube (High M_g) => Nucleation	Rot. Cube (Low M_g) => SIBM Cube (High M_g) => Nucleation
Shared zones (K ≅ 1)	γ fiber (Low M_g) => SIBM	(1) α* fiber (High M_g) => Nucleation (2) γ fiber (Low M_g) => SIBM

Regarding the obtained figure for the image quality plus the rotation angle map (misorientation) of sample 1 and sample 2 after annealing at 700 °C, 760 °C and 800 °C for 20 s, see Figure **16**, we observe fragmentation in the deformation bands during annealing at 700 °C and finally nucleation at 760 °C for sample 1. For sample 2 we get first recovery in deformation bands and recrystallization in bands with large shear lines (shear bands) at annealing at 700°C. More or less complete recrystallization is observed for annealing at annealing temperatures above 760 °C. Considering these observations we may conclude that the responsible mechanism at recrystallization for our feritic FeSi samples comprise nucleation as well as SIBM, as summarized in Table **2**.
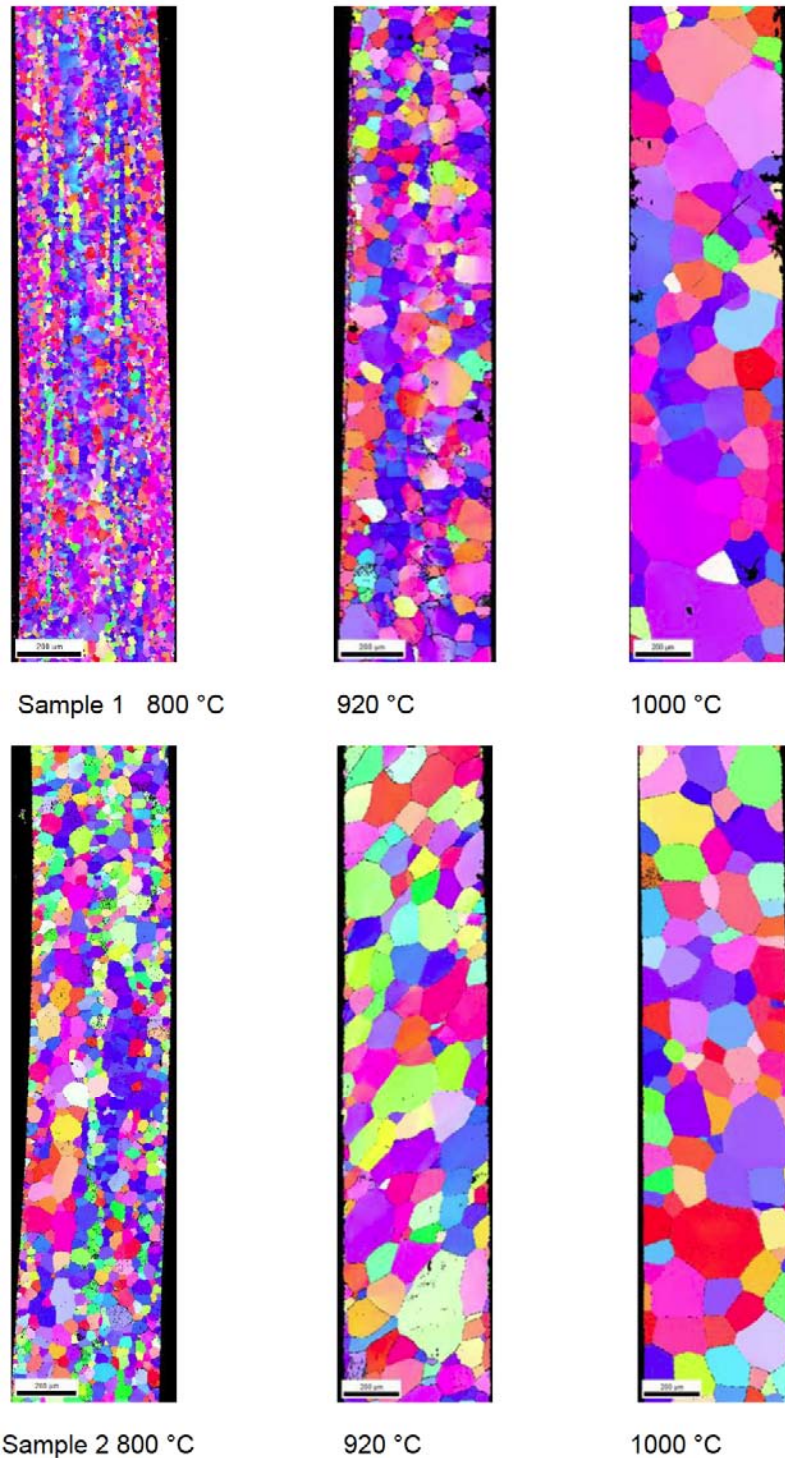
Figure 22: OIM of sample 1 and 2 after annealing for 20 s at higher temperatures.

3.2.2. Annealing at High Temperatures

There is a strong link between the specific magnetic losses of the fully processed electrical steel and its microstructural features, especially the grain size. Large values of grain size are necessary to reach low values of the specific magnetic losses. To reach large grain size a final annealing at high temperatures is necessary to obtain grain growth, which follows the recrystallization at final annealing of the cold rolled material. We follow the definition in [11], where grain growth is defined as grain coarsening after completed recrystallization (stress less polycrystalline microstructure). Of special interest for the regarded non-oriented ferritic FeSi steels is the evolution of the grain structure and texture at annealing temperatures above 800 °C, where we have grain growth instead of recrystallization.

In the following, we regard the microstructure and texture after annealing at different temperatures in the range of 800 °C up to 1050° C with fixed annealing time of 20s of the samples 1, 2, 7. These selected samples exhibit typical figures for the microstructure of hot strips: sample 1 rapidly quenched after the last pass at hot rolling, sample 2 thermal annealed after the last pass at hot rolling, and sample 7 annealed in a separate processing step before cold rolling. Figures **22** and **23** present the orientation imaging microscopy map (OIM) of sample 1 and 2, respectively 3 and 7 after annealing at higher temperatures.

Although the deformation at cold rolling was the same for all samples we observe a different behavior. The evaluation of the microstructure and texture at annealing at temperatures, where grain growth is going on, depends on the type of the used hot band. While for sample 2 and 7 the recrystallization is practically completed for an annealing at 800°C, sample 1 is even not completely recrystallized after annealing at 800 C° for 20s. As can be seen from the Figures for the OIM the image of the texture as well as the grain structure changes remarkable as the grain growth is going on at annealing at higher annealing temperatures. Thereby the appearance of the texture as well as of the grain structure is different for hot bands with different microstructure. Even different hot band annealing results in different behavior, see Figure **22** (sample 2) and Figure **23** (sample 7).

The changes of the image of the texture for the samples 1, 2 and 7 can be seen more clearly from Figures **24** and **25**. The highest intensities for the preferable magnetic texture components are obtained for sample 2 and 7. Optimum annealing temperature for maximum intensity of preferable magnetic texture seems to be different, depending on the microstructure of the hot band.

The evolution of texture at grain growth depends sensitively on the microstructure of the hot band as well as on the annealing parameters T and t. The changes of the microstructure and texture for annealing at a

800 °C   870°C   920°C   1000°C   1050 °C
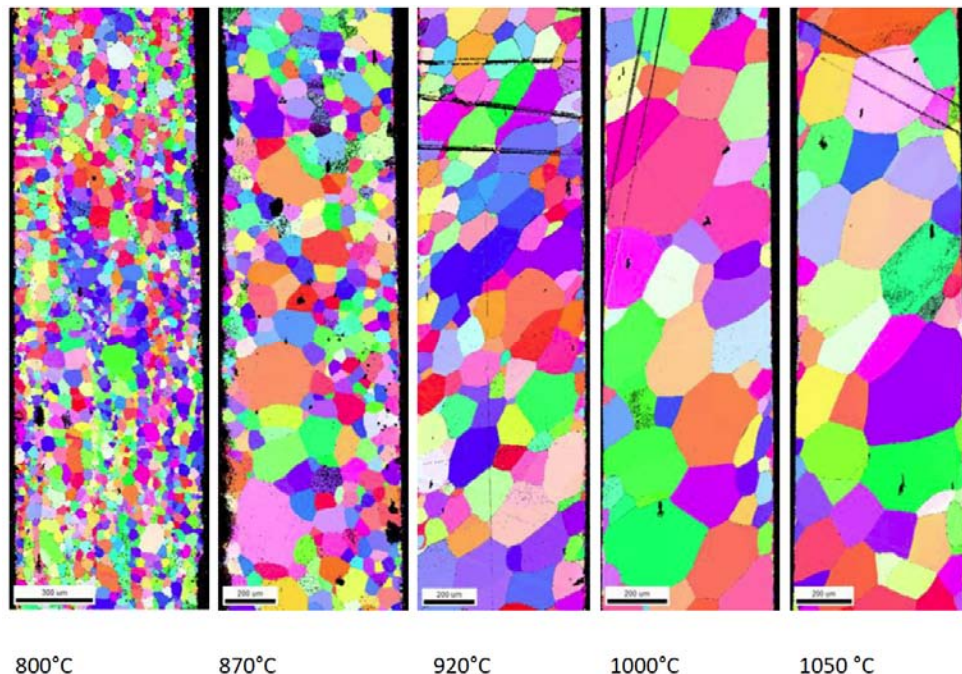
Figure 23: OIM of sample 7 after annealing at higher temperatures for 20s.

(a) sample 1; 800°C / 20 s

(b) sample 1; 920°C / 20 s

(c) sample 1, 1000°C / 20

(d) sample 2, 800°C/20s

(e) sample 2; 920°C / 20 s

(f) sample 2; 1000°C / 20 s
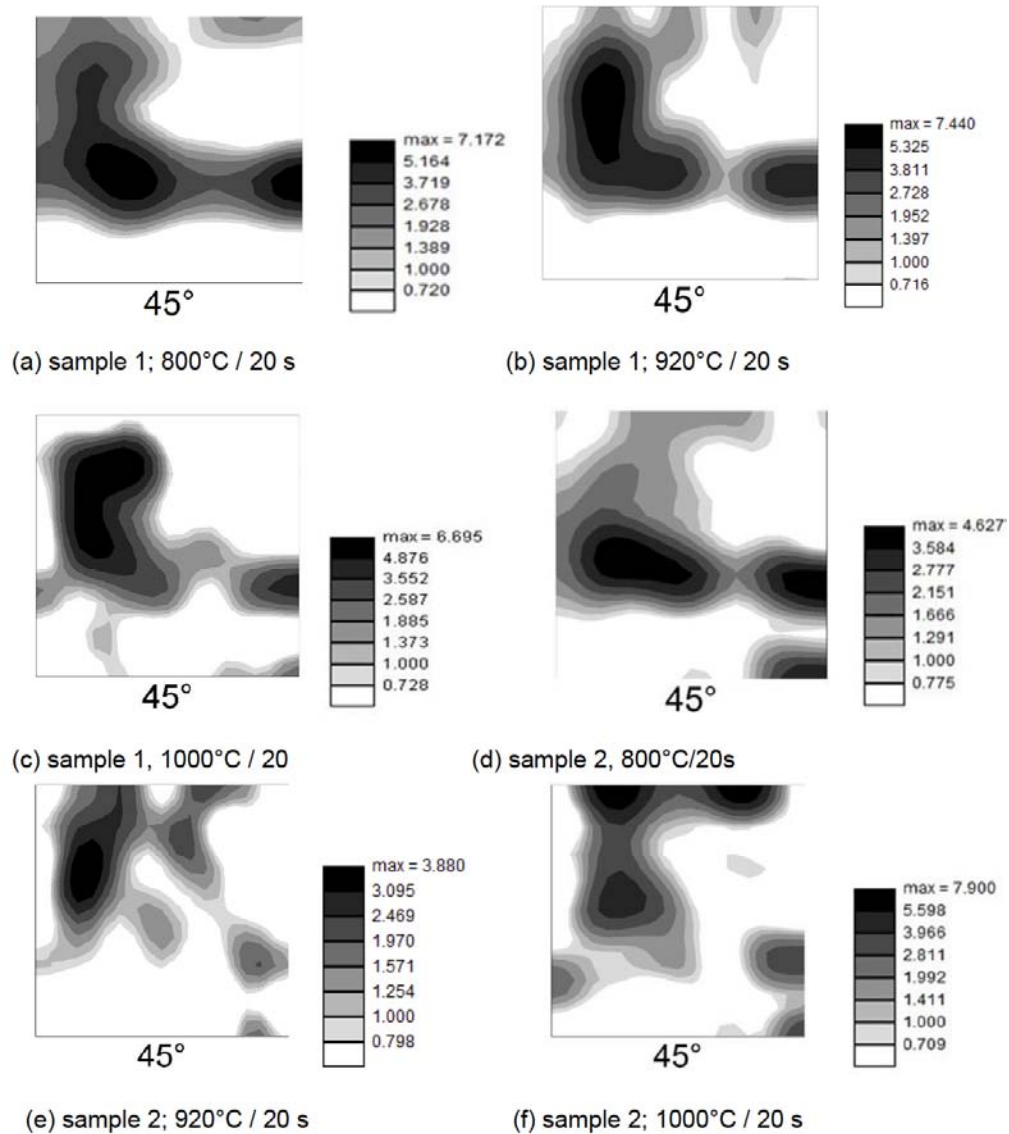
Figure 24: ODF section φ_2=45° (total) after final annealing at different temperatures for 20 s: sample 1 - (**a**), (**b**), (**c**) and sample 2 - (**d**), (**e**), (**f**).

given temperature, where the annealing time is increased, is shown in Figure **26**. The Figures present the OIM and the ODF for sample 1 and sample 2 at annealing at 750 °C for different annealing temperatures. Depending on the type of hot band there is also an optimum annealing time at a given annealing temperature for optimum magnetic texture components.

The obtained data seem to indicate that above the optimum value of the annealing temperature, respectively the annealing time, the intensities of the preferable texture components appear to decrease, while the grain size is still increasing. More intensive investigation is necessary to validate this statement. Thereby one has to taken into account that the ODFs

obtained from EBSD measurements are normally done for a magnification of 100. This may not be representative for the whole band. The evolution of the grain structure and texture is heterogeneous along the length of the band, as demonstrated in Figure **27** for sample 7 after annealing at 1050 °C for 20s, see also [17].

While at the primary recrystallization the stored deformation energy gives the driving force, the grain growth is determined by the grain boundary energy. Grain boundary energy is not homogeneous and may be different for a grain with different neighboring grains. The character of the misorientation between neighboring grains gives the boundary character. The misorientation determines the difference in energy.
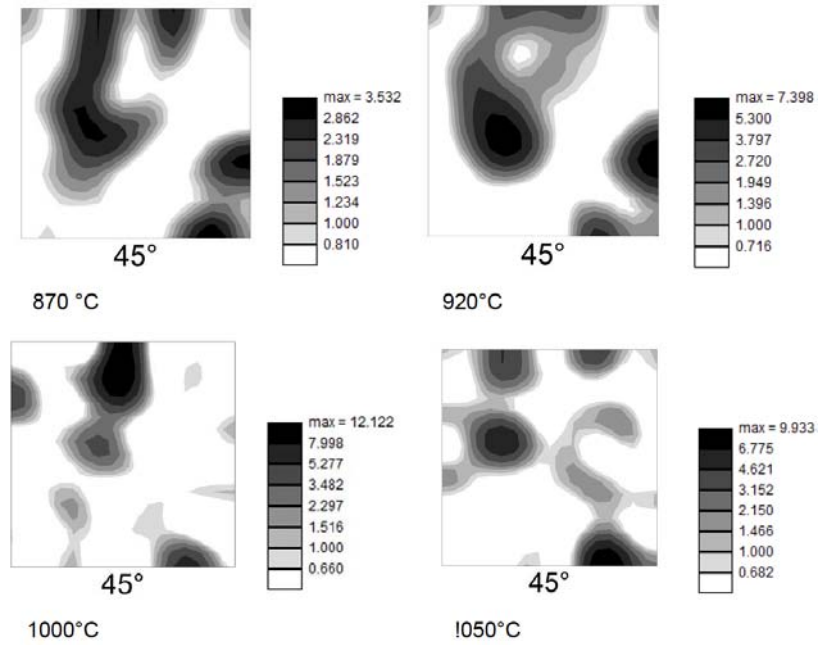
Figure 25: ODF section φ$_2$=45° of sample 7 after final annealing at different temperatures for 20 s.
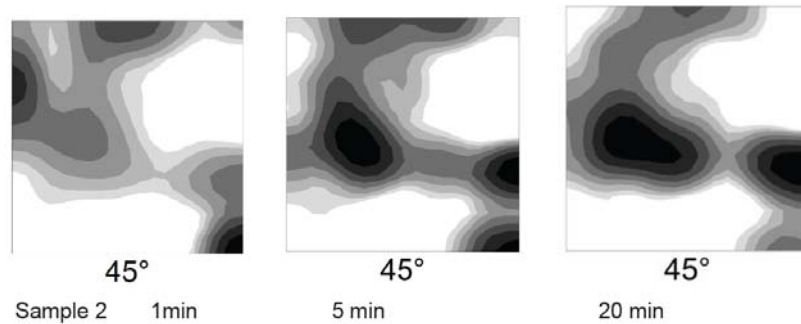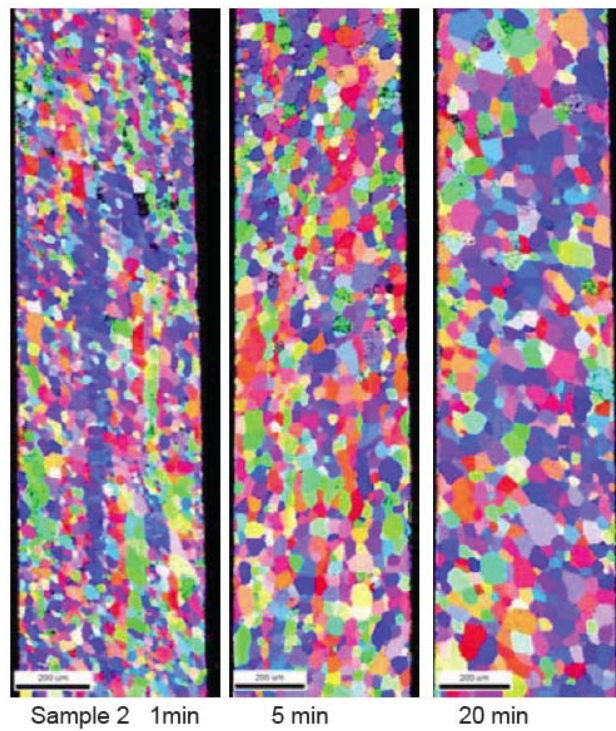
Figure 26: OIM and ODF section φ$_2$=45° of sample 2 after annealing at T= 750°C for different time annealing time.
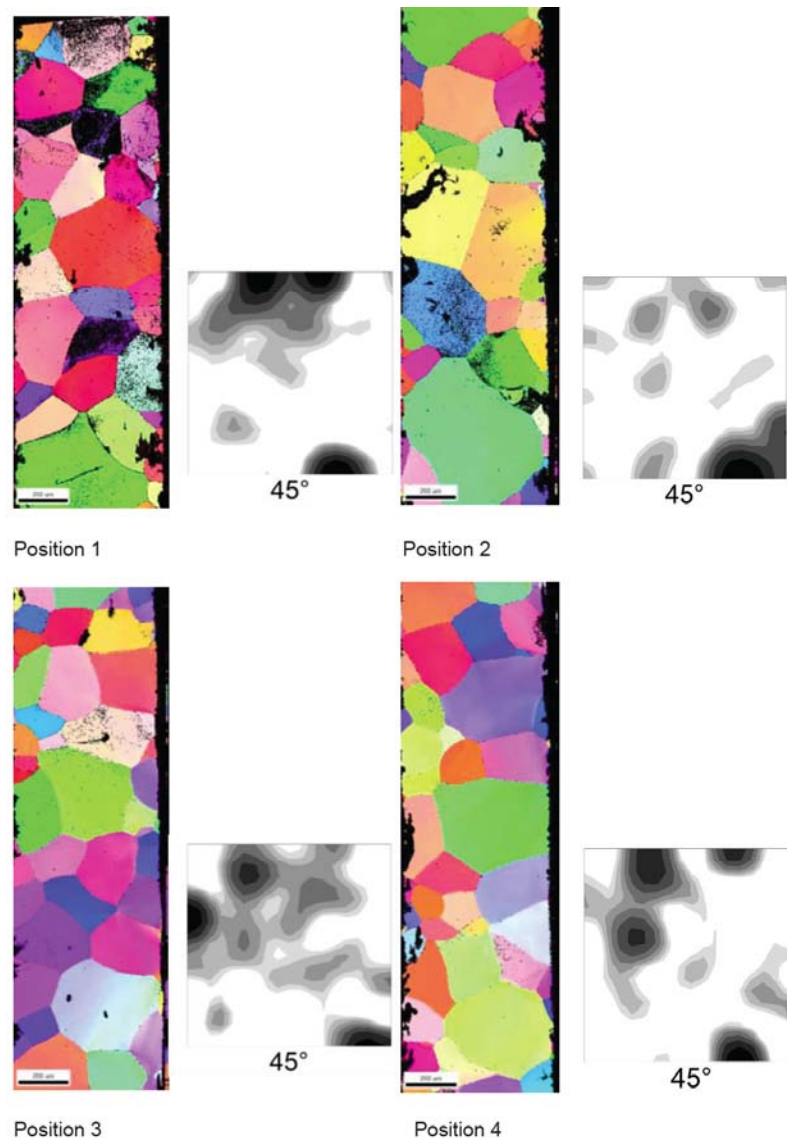
Figure 27: OIM and ODF of sample 7 after annealing at 1050 °C for 20 s vs. various positions along the length.

At pesent there are no data for the energy ranking of GBs due to different misorientation between neighboring grains. This energy ranking may give rise to selective grain growth with respect to the texture. The diffusity may be affected by precipitations or even by localized stresses.

CONCLUSIONS

It is well established that there is an interplay and interaction between the processing steps at fabrication of non-oriented electrical steels: hot rolling, cold rolling and annealing with respect to the evolution of the microstructure and texture.

Depending on the microstructure of the hot band a rather complex deformation structure appears for ferritic FeSi steels after the heavy cold rolling to reach the desired final thickness. This complex deformation structure affects the ongoing recrystallization and finally the grain growth at final annealing. Thereby the microstructure of the hot band determines the start of the recrystallization and finally the start of the grain growth at final annealing. Optimized properties (low magnetic losses) needs large grain size, for which grain growth at final annealing is necessary.

At annealing of the cold rolled strips with high deformation at first recovery and recrystallization appear. The texture evolution at recrystallization cannot be described only by regarding in-plane compression stress. Present shear stress changes the appearance of texture at recrystallization.

At higher annealing temperatures, finally grain growth is going on. The evolution of texture at grain

growth is different from those at recrystallization. Optimum intensity of preferable magnetic textures are obtained for hot strips, which were thermal annealed after the last pass at hot rolling or in a separate processing step before final annealing. The kinetic for the evolution of texture at grain growth may depend sensitively on the microstructure of the hot band as well as on the annealing parameters T and t.

While the grain size increase with increasing the annealing temperature or the annealing time, the image for the texture changes. One has to taken into account that for the primary recrystallization the stored deformation energy gives the driving force, while the grain growth is determined by the grain boundary energy (GB energy). GB energy is not homogeneous and may be different for a grain of a given size with different neighboring grains.

This energy ranking may give rise to selective grain growth with respect to the texture. However, there are no data for the regarded non-oriented ferritic FeSi steels.

The present models of the evolution of the microstructure and texture along the processing route like for instance SCORE - Statistical Cellular Operator and the Level-Set-Modell, which starts from the hot band microstructure and which comprise the cold rolling and final annealing, fails to predict the evolution of microstructure and texture for the regarded ferritic FeSi steels. One may fit the experimental data, however a prediction of the resulting grain size and of the intensities of texture depending on the process parameters is not possible. The pre-conditions of the model are not fulfilled (no well-defined grain structure of the hot band; much higher deformation at cold rolling; microstructure after cold rolling cannot be described as "deformed grains").

REFERENCES

[1]   Gomes E, Schneider J, Verbeken K, Hermann H, Houbaert Y. Mater Sci Forum 2010; 638-642: 3561-3566.
https://doi.org/10.4028/www.scientific.net/MSF.638-642.3561

[2]   Verbeken K, Schneider J, Verstraete J, Hermann H, Houbaert Y. IEEE Trans on Magn 2008; 44: 3820.
https://doi.org/10.1109/TMAG.2008.2001318

[3]   Schneider J, Franke A, Stöcker A, Liu H-T, Wang G-D, Kawalla R. IEEE Trans on Magn 2016; 52: 1-6.
https://doi.org/10.1109/TMAG.2016.2530147

[4]   Franke A, Schneider J, Bacroix B, Kawalla R. Journal of Material Science and Technology Research 2018; 5: 28-38.
https://doi.org/10.1109/TMAG.2016.2530147

[5]   Franke A, Schneider J, Stöcker A. Proc. 7. International Conf. Magnetism and Metallurgy WMM18, June Rome, Italy 2016; p. 325. ISBN 9788890003301

[6]   Schneider J, Franke A, Stöcker A, Kawalla R. Steel Research Int 2016; 87(8): 1054.
https://doi.org/10.1002/srin.201500447

[7]   Schneider J, Stöcker A, Franke A, Kawalla R. AIP Advances 2018; 8: 047606.
https://doi.org/10.1063/1.4993526

[8]   Schneider J, Franke A, Kawalla R. Proc. 8. International Conf. Magnetism and Metallurgy WMM18, June Dresden, Germany Part II, 2018; pp. 612-629. ISBN 978-3-86012-579-3

[9]   Calvillo PR, Schneider J, Houbaert Y. Characterization of Flat Rolled High-Silicon Steel by EBSD, Defect and Diffusion Forum Online: 2009-03-02 ISSN: 1662-9507, Vols. 283-286, 413.
https://doi.org/10.4028/www.scientific.net/DDF.283-286.413

[10] Hutchinson B. Deformation Substructures and Recrystallization. Mat Science Forum 2007; 668: 13.
https://doi.org/10.4028/www.scientific.net/MSF.558-559.13

[11] Gottstein G. Physikalische Grundlagen der Materialkunde, Springer Berlin Heidelberg 2007.

[12] Raabe D. Physical Metallurgy, 5th Edition, Elsevier 2014; p. 2291.
https://doi.org/10.1016/B978-0-444-53770-6.00023-X

[13] Yasihiki H, Okamoto A. Effect of hot band grain size on magnetic. IEEE Transactions on magnetics 1987; 23(5): 3086-3088.
https://doi.org/10.1109/TMAG.1987.1065261

[14] Huneus H, Günther K, Kochmann T, Plutniok V, Schoppa A. Journal of Materials Engineering and Performance 1993; 2(2): 199-203.
https://doi.org/10.1007/BF02660286

[15] Schneider J, Franke A, Stöcker A, Kawalla R. Journal of Electrical Engineering 2018; 69(6): 458-460.
https://doi.org/10.2478/jee-2018-0074

[16] Dorner D, Zaefferer S, Raabe D. Acta Materiialia 2007; 55: 2519.
https://doi.org/10.1016/j.actamat.2006.11.048

[17] Kestens L, Ngyuyen-Minh T, Sidor JJ. Proc. 7. International Conf. Magnetism and Metallurgy WMM18, June Rome, Italy 2016; p.197, ISBN 9788890003301

[18] Sidor JJ, Verbeken K, Gomes E, Schneider J, Calvillo PR, Kestens LA. Mat Characterization 2012; 71: 49-57.
https://doi.org/10.1016/j.matchar.2012.06.006

[19] Ray RK, Jonas JJ, Hook RE. International Materials Review 1994; 39(4): 129.
https://doi.org/10.1179/imr.1994.39.4.129

[20] Kestens L. Modern Theories on Plastic Deformation of Metals, Nov. 17 2008; TU-Delft.